Magnetotransport in the rare earth silicides RSi_{2-x}

1994 J. Phys.: Condens. Matter 6 79

(http://iopscience.iop.org/0953-8984/6/1/010)

J. Phys.: Condens. Matter 6 (1994) 79–92. Printed in the UK

Magnetotransport in the rare earth silicides RSi_{2-x}

J Pierre†, S Auffret†‖, J A Chroboczek‡ and T T A Nguyen§

† Laboratoire L Néel, CNRS, 166X, 38042 Grenoble, France
‡ Centre N Ségard, CNET, 38243 Meylan, France
§ LEPES, CNRS, 166X, 38042 Grenoble, France

Received 17 June 1993, in final form 18 October 1993

Abstract. The resistivity, magnetoresistance and Hall effect of the rare earth silicides RSi_{2-x}, with x from 0 to 0.4, have been measured on several polycrystalline samples, single crystals and epitaxial thin films. All samples are metallic; the Hall effect measured for some phases shows that we are dealing with nearly compensated metals. The magnetoresistance displays peculiar features in antiferromagnetic phases, which are explained by the increase of spin disorder scattering at the metamagnetic transition.

1. Introduction

Transition metal silicides TSi_2 have been well known for a long time and are presently used in many microelectronic devices, as they form epitaxial layers on silicon [1]. They can be used in low-resistivity metallic contacts, diodes or metallic base transistors [2]. The study of their thermoelectric properties has revealed high values of the Seebeck coefficient particularly for $MnSi_2$ and $MoSi_2$ [3].

Rare earth silicides may also form epitaxial layers on Si [4]. These stable, metallic phases can also be promising for applications. $ErSi_{2-x}$ on Si may be used in high-quality diodes [5], as well as infrared detectors [6].

In order to develop applications, a better knowledge of the transport properties of silicides is required. The present paper focuses on the electrical transport properties of rare earth silicides as bulk or thin-film materials. The thermopower has also been measured and will be described in a forthcoming paper.

The crystallographic properties have been described earlier in several papers [7, 8]. Three main crystallographic structures are encountered, depending on the rare earth metal and on the silicon content: the tetragonal $ThSi_2$ structure, its distorted orthorhombic variants $GdSi_{2-x}$, and the hexagonal AlB_2 structure. The latter is found mainly in heavy rare earth compounds for a stoichiometry close to R_3Si_5, and corresponds to the structure of epitaxial films grown on Si ⟨111⟩.

The magnetic properties and magnetic structures have also been thoroughly investigated [9–12].

‖ Present address: Département de Recherches Fondamentales, Centre d'Etudes Nucléaires, 85X, 38041, Grenoble, France.

0953-8984/94/010079+14$07.50

2. Experimental methods

Bulk samples were obtained at the L Néel Laboratory, using induction melting in a copper water cooled crucible, and the Czochralski method in the same kind of crucible was used to obtain single crystals.

$ErSi_x$ epitaxial layers were obtained by molecular beam epitaxy on intrinsic Si at the CNET Meylan, whereas $TbSi_x$ layers were obtained at the LEPES laboratory by a codeposition of the elements on Si, followed by annealing at 600 °C.

The resistivity was measured by the AC current four-probe method, from 1.5 to 300 K, under fields of up to 6.5 T. The Hall effect was measured by the Van der Pauw method on square platelets. The magnetic field was reversed in order to separate the magnetoresistance from the Hall contribution. The Hall voltage is then $V_H = [V(H+) - V(H-)]/2$; this procedure also allows us to eliminate the spurious term due to the misalignment of voltage electrodes.

3. Resistivity

3.1. Phonon resistivity

The resistivity has been measured on non-magnetic La and Y compounds. Previous measurements on $LaSi_{1.75}$ (tetragonal) and $YSi_{1.7}$ (hexagonal) single crystals show some anisotropy in the resistivity [13]. The phonon slope is larger (by about 20%) for the current along the c axis for $YSi_{1.7}$ and slightly larger for the current along the a axis for $LaSi_{1.75}$.

Measurements on a $YSi_{1.7}$ polycrystal show a low temperature dependence as $T^{4\pm0.3}$ up to 30 K. A good overall fit with a Bloch–Grüneisen law is observed up to room temperature (figure 1). The Bloch-Grüneisen formula is written as

$$R(T) = R_0 + A(T/\Theta)^n J_n(\Theta/T) \qquad J_n(x) = \int_0^x \frac{z^n \, dz}{(e^z - 1)(1 - e^{-z})}$$

where we take $n = 4$. We obtain a Debye temperature $\Theta_D = 380 \pm 30$ K; this value agrees with specific heat data of Sato *et al* [14], which give $\Theta_D = 400$ K.

The resistivity of polycrystalline $LaSi_{1.9}$ has been measured; it displays specific features: first a superconducting transition is observed at 3 K, which had already been observed by Sato *et al* for stoichiometric $LaSi_2$ at 2.3 K [14].

A second anomaly is observed in the slope of the resistivity between 150 and 200 K (figure 1). This anomaly, which displays some hysteresis, is ascribed to a change in the crystallographic structure. Similar behaviour has been observed in $CeSi_x$ and $PrSi_x$ compounds in this temperature range [15]. Starting from a single tetragonal phase at room temperature, the samples undergo a transformation that gives rise to a mixture of two phases. One at least shows superstructure Bragg reflections, related probably to vacancy ordering on the Si sites. This structural transformation seems quite general in light rare earth compounds, for Si content between 1.8 and 1.9. It is absent in the orthorhombic phase of $LaSi_{1.75}$, and does not occur in the magnetic samples described hereafter.

A fit of the data obtained below 120 K by a Grüneisen law gives a Debye temperature of 240 ± 20 K. This agrees with the value (252 K) obtained from specific heat measurements by Dijkman [16], but is much lower than the value obtained by Sato *et al* for stoichiometric $LaSi_2$ [14], which is 365 K. No crystallographic transformation was indeed reported for this 1:2 composition. Thus the low Debye temperature may be related to soft phonon modes involved in the crystallographic transformation.

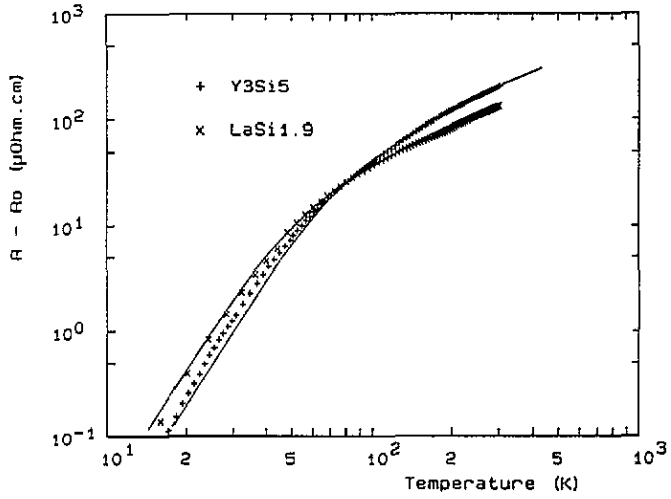

Figure 1. Resistivity less residual value as a function of temperature for $YSi_{1.67}$ and $LaSi_{1.9}$. Continuous lines are fits to Bloch–Grüneisen laws (below 120 K for $LaSi_{1.9}$). The residual value is 23 $\mu\Omega$ cm for $YSi_{1.7}$ and 33 $\mu\Omega$ cm for $LaSi_{1.9}$ (at 3 K).

3.2. Magnetic resistivity

The resistivity for magnetic phases displays several distinct features related to magnetic ordering and magnetic transformations in the ordered range, and slope changes in the paramagnetic range related to crystal field effects. We do not describe all of them, as some have been analysed before [10, 17], but only give some preeminent features. We particularly emphasize the spin disorder contribution in paramagnetic and ordered magnetic structures.

When the crystal field level scheme is known as for instance in $NdSi_{1.8}$, through the anisotropy of the susceptibility and neutron inelastic scattering [18], the magnetic resistivity can be reproduced within the van Peski-Tinbergen–Dekker (VPD) theory [19]. According to their theory, the resistivity is written as

$$R_m = R_m^{\infty} \mathrm{Tr}(\mathbf{PQ})$$

where $\mathbf{P}$ and $\mathbf{Q}$ are symmetrical matrices depending on the energy of crystal field levels and matrix elements between them. R_m^{∞} is the magnetic resistivity for $T \to \infty$.

$$P_{ij} = p_i[(E_j - E_i)/k_B T]/\{1 - \exp[-(E_j - E_i)/k_B T]\}$$

where E_i and p_i are respectively the energy and Boltzmann factor for each crystal field level.

The VPD expression for Q_{ij} derived in the paramagnetic range may be generalized in order to include the reduction of spin disorder due to the spontaneous magnetization in the ordered range.

Assuming a collinear magnetic structure with the magnetization defined by the two components $M_z = g\langle J_z\rangle$ and $M_x = g\langle J_x\rangle$, the matrix elements of $\mathbf{Q}$ are then

$$Q_{ij} = |\langle i|J_z|j\rangle - \langle J_z\rangle\delta_{ij}|^2 + |\langle i|J_+|j\rangle - \langle J_x\rangle\delta_{ij}|^2 + |\langle i|J_-|j\rangle - \langle J_x\rangle\delta_{ij}|^2$$

where $\langle i|J_\alpha|j\rangle$ are the matrix elements between levels, and $\delta_{ij} = 1$ if $i = j$, and 0 otherwise.

In the paramagnetic range, $\langle J_z\rangle = \langle J_x\rangle = 0$, we recover the expression of van Peski-Tinbergen and Dekker.

In order to obtain eigenvalues and eigenvectors, the Hamiltonian containing crystal field and exchange components is first diagonalized in a self-consistent manner, incorporating the crystal field parameters obtained from magnetic and neutron data and the value of ordering temperature.

An example is given in figure 2(*a*), which represents the resistivity derivative for the $NdSi_{1.7}$ ferromagnetic compound along the *a* and *c* axes. The resistivity itself is nearly isotropic, apart from a slightly different value of the residual term. This isotropic character is maintained in the ordered range, whereas the magnetic anisotropy is large with the magnetization confined in the basal (a, a) plane of the tetragonal structure. We may thus neglect anisotropic terms in the resistivity, such as the quadrupolar terms described by Fert *et al* [20]. It is well known that as the magnetic resistivity is linked to the magnetic disorder (entropy), its derivative will exhibit features analogous to the specific heat, that is Schottky anomalies associated with the thermal population of excited crystal field levels, and a lambda type anomaly at the ordering point.

Figure 2(*b*) is a fit obtained by taking the crystal field parameters [18] as explained before, and adjusting the exchange parameter to fit the Néel temperature. The fit accounts correctly for the Schottky like anomaly near 15 K, associated with the population of crystal field excited levels. The fit is not so good in the ordered range: the mean field theory is not exact, and for instance does not describe properly the occurrence of spin wave gaps at low temperature. Also the magnetic structure may not be collinear in the vicinity of the ordering point, which causes an increase of the resistivity due to the structure modulation and the onset of magnetic gaps on the Fermi surface [21]. We do not take this phenomenon into account in the following.

When the crystal field is not known, except for the degeneracy N of the ground state (which is the case in most compounds), the variation of the magnetic resistivity in the ordered range is related to this degeneracy, as the entropy increases more smoothly for larger N. The VPD theory may give this temperature dependence of the resistivity for a pseudospin with the degeneracy $N = 2S + 1$. A different approach has been followed by Yamada and Takada [22], who compute the magnetic resistivity and magnetoresistance for a classical spin S. The numerical results obtained from the two theories are slightly different. The reduced magnetic resistivity $R(T)/R(T_N)$ as a function of reduced temperature T/T_N for some silicides is given in figure 3 [11, 17]. The temperature dependence has a positive curvature largest for those ions with a small ground state degeneracy (for instance Tb_3Si_5 with a doublet ground state), whereas its variation shows a more linear behaviour or even a negative curvature for $GdSi_x$ compounds, due to the progressive entropy gain by the thermal population of the $(2J + 1) = 8$ levels. For $ErSi_{1.67}$, the temperature dependence has an intermediate behaviour, related to a quasifourfold ground state degeneracy.

4. Magnetoresistance

The magnetoresistance has been studied for some single crystals and thin films with different current/field geometries. A peculiar behaviour was observed in metamagnetic compounds, leading to a sharp maximum in the resistance for the critical field of metamagnetism. Such a phenomenon has been previously described for instance in thin films Er_3Si_5 [17].

This behaviour had already been observed much earlier in pure rare earths themselves [23], and explained by Yamada and Takada [22]. In the following, we will use their theory

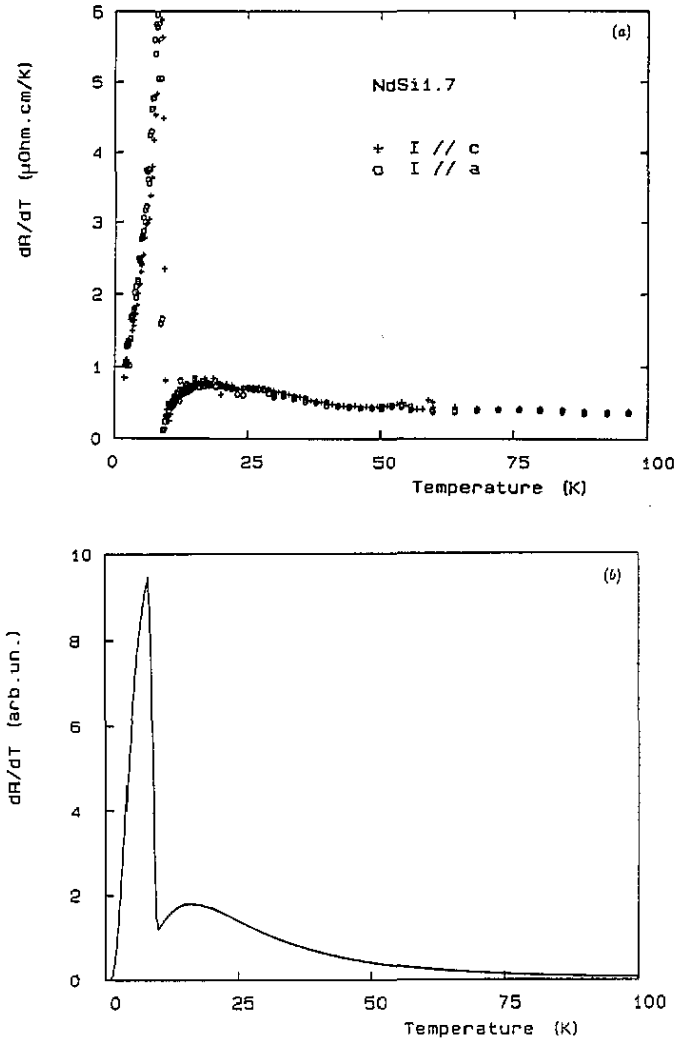

Figure 2. (*a*) Temperature derivative of the resistivity for ferromagnetic $NdSi_{1.7}$. (*b*) Fit using crystal field + mean field model.

derived for a classical spin, and extend it to the case of crystal field split ions by describing the metamagnetic behaviour within a (crystal field + exchange) mean field Hamiltonian, and incorporating the resulting values for energies and moment directions.

It is worthwile to give first a simple phenomenological description for the magnetoresistance for ordered magnets. De Gennes and Friedel [24] gave the expression of the magnetic resistivity as a function of the spin correlation function $\langle S_i S_j \rangle_T$. Applying this to a spin doublet $\pm\mu$, the magnetoresistance in the paramagnetic range varies as $\tanh^2(\mu H/kT)$. More generally, the scattering of conduction electrons depends on the ratio $\Delta E/kT$, where ΔE is the magnetic splitting; it decreases as a function of this splitting in the ferromagnetic range (figure 4, left). The shape of the magnetoresistance in the ordered range may be deduced approximately from the curve in the paramagnetic range by a horizontal shift corresponding to the exchange field H_{ex}, at least for an isotropic ferromagnet. The VPD

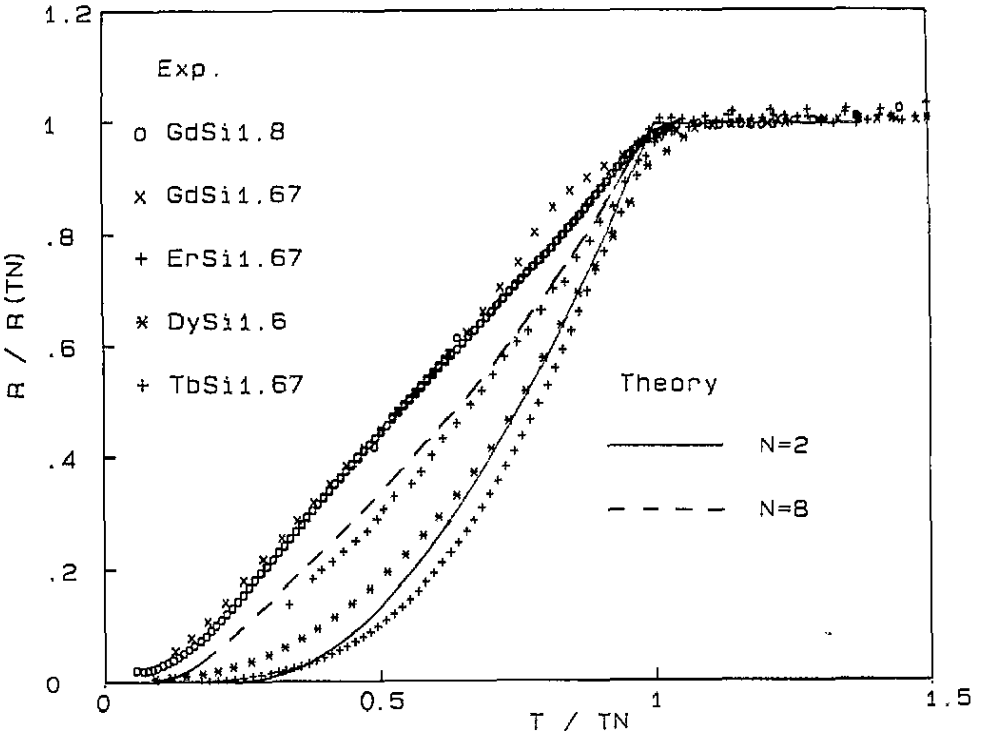

Figure 3. Reduced magnetic resistivity for various silicides versus reduced temperature T/T_N. The temperature dependence is compared to theoretical calculations using the Yamada–Takada model, with degeneracies $N = 2$ and 8 of the ground state.

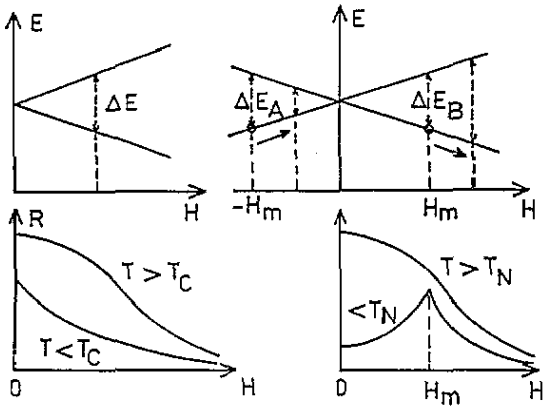

Figure 4. Schematic behaviour of the ground state splittings and spin-disorder resistivity: a ferromagnetic system (left) and a two-sublattice Ising antiferromagnet with the field H applied along the common spin direction (right).

theory may be extended to this case, but calculations in other cases (anisotropic ferromagnet, antiferromagnet and metamagnet) require a tedious Green function calculation.

Let us now consider a simple Ising like antiferromagnet. Applying the field along

the common direction of spins gives rise to an increase of the magnetic splitting ΔE_B of the upward sublattice (B), whereas a decrease of the splitting occurs for the downwards sublattice (A) up to the reversal of the total field ($H - H_{ex}$) on this sublattice (figure 4, right). At this point, the scattering of conduction electrons on the A site is largest, giving a maximum in the resistivity, and decreases on increasing the applied field further. Conversely, applying the field perpendicularly to the direction of spins leads to a progressive decrease of the resistivity.

Such 'cusps' in the magnetoresistance have been observed in some silicides or arsenides [25], and may help to draw the magnetic phase diagram of antiferromagnets.

This behaviour has been clearly observed for Er_3Si_5, where the magnetic structure allows us to separate the behaviour for a field parallel or perpendicular to the axis of antiferromagnetism. Due to crystal field and anisotropic exchange interactions, components of moments perpendicular to the c axis ($3\mu_B$) are aligned ferromagnetically, whereas components parallel to c ($7\mu_B$) are ordered antiferromagnetically. This structure deduced from neutron data [17] is in line with magnetization data obtained on single-crystal material or thin films. The structure undergoes a metamagnetic transition when a field larger than 1.5 T is applied along the c axis. The magnetoresistance of a thin $ErSi_{1.7}$ film is given in figure 5 for H parallel or perpendicular to the film.

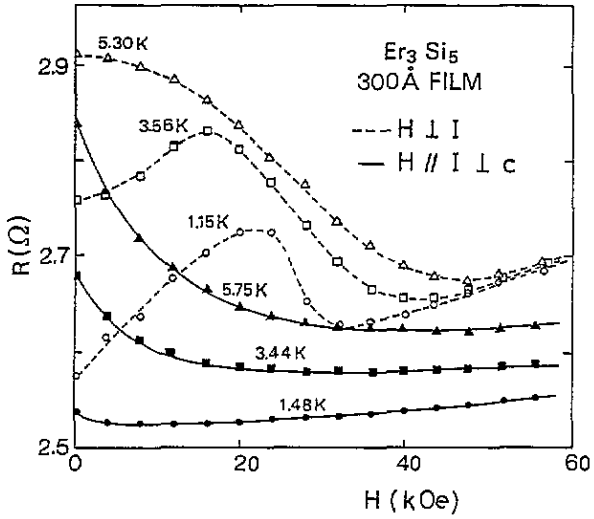

Figure 5. Magnetoresistance of an $ErSi_{1.7}$ epitaxial film with the field applied in the plane parallel to the current, or perpendicular to the film, from [17].

Yamada and Takada [22] have analysed the magnetoresistance of simple antiferromagnets when the field is applied parallel or perpendicular to the direction of spins. They assume classical spins, with a small uniaxial anisotropy. They decompose the magnetic resistivity into two contributions, related to the transverse and longitudinal modes of spin fluctuations. The resistivity is written as

$$R_m = R_{long} + R_{trans}$$

where

$$R_{long} = K\partial\mu/\partial(E/k_BT)$$

and

$$R_{\text{trans}} = K(\mu E/2k_{\text{B}}T)/\sinh^2(E/2k_{\text{B}}T).$$

E is the magnetic energy (sum of molecular field and Zeeman terms), and μ the magnitude of the magnetic moment at the temperature of the experiment. For a simple antiferromagnet, the scattering matrix can be decoupled into a sum on the two sublattices A and B; thus the resistivities themselves are expressed as sums on the two sublattices.

It is possible to generalize their theory to the case of crystal field split ions in the following way: the mean field Hamiltonian containing crystal field, molecular field and Zeeman terms is diagonalized in a self-consistent manner for each field and temperature. For a simple antiferromagnet, the Oz axis is taken as the common direction of spins in zero field, the field direction being either along Oz or Ox. The components M_z and M_x are computed self-consistently for each sublattice, as well as the magnetic energy, which is defined as $-M(H + H_{\text{m}})$. The longitudinal resistivity, associated with the derivative of the moment versus total field on the sublattice, is calculated numerically giving a small increment to the applied field, which requires reaching a good convergence in the self-consistent calculation.

Numerical fits for Er_3Si_5, using crystal field parameters and exchange parameters deduced from susceptibility, ordering point and neutron inelastic scattering measurements [17], are given in figure 6, and agree qualitatively with experimental data.

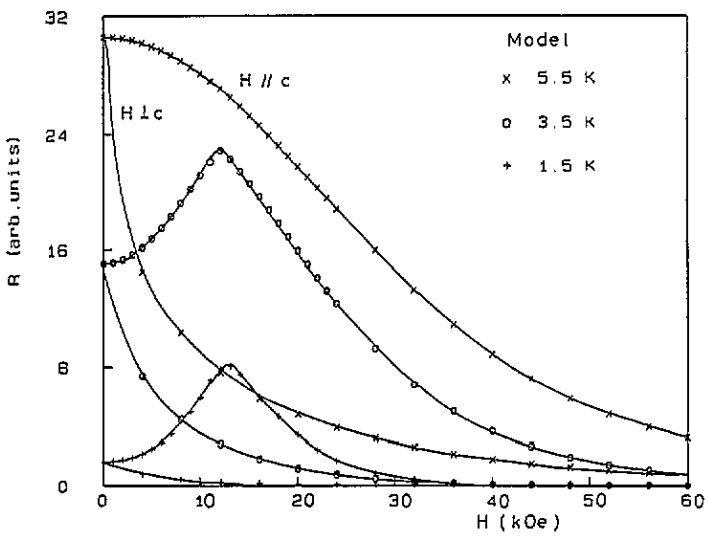

Figure 6. Theoretical variation of the magnetoresistance of $ErSi_{1.7}$ in a crystal field + mean field model (see text).

As another example, we give in figure 7 the longitudinal magnetoresistance for a single crystal of $NdSi_{1.8}$, with the field and current aligned along the (100) axis.

In the case of $NdSi_{1.8}$, which is antiferromagnetic below 10 K in contrast to ferromagnetic $NdSi_{1.7}$, the problem is complicated by the fact that this nearly tetragonal compound has different antiferromagnetic domains, with spin directions along the [100] or [010] axis, which gives rise to spin flopping when the field is applied in the basal plane.

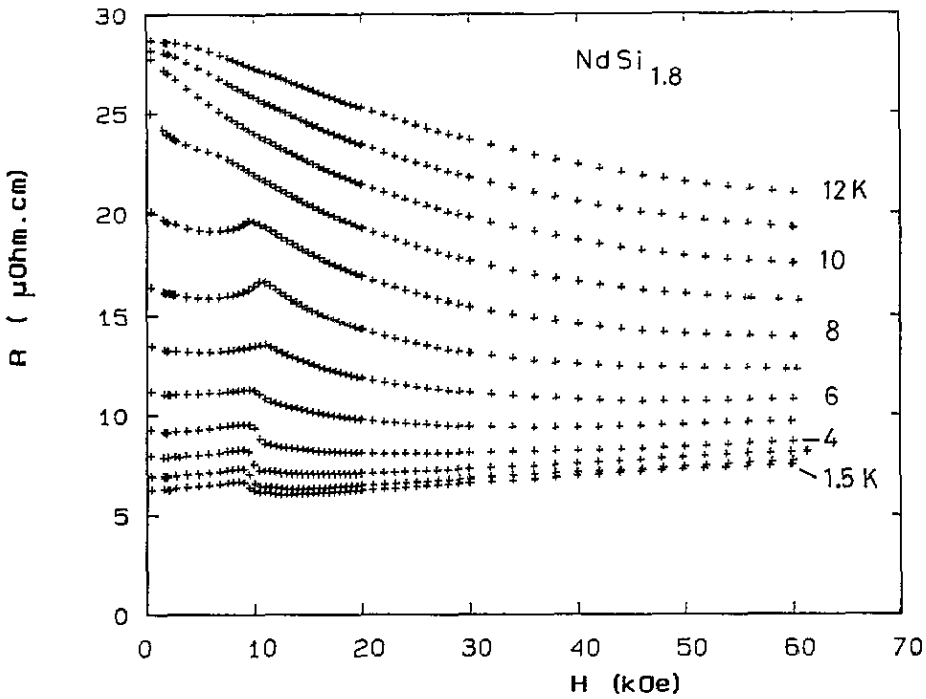

Figure 7. Magnetoresistance for an antiferromagnetic $NdSi_{1.8}$ single crystal, demonstrating the phase diagram of the metamagnetic transition.

This fact blurs the more simple behaviour obtained for the Er compound, and decreases the amplitude of the cusp observed when the field is applied in the basal plane.

We also see in figures 5 and 7 that the resistivity for the ferromagnetic state extrapolated to vanishing field is indeed smaller than the actual resistivity for the antiferromagnetic phase. This discrepancy is related to the influence of carrier scattering by the additional Brillouin zones [21].

5. The Hall effect

The Hall effect had been measured previously on thin epitaxial films of $YSi_{1.7}$ [26] and $ErSi_{1.7}$ [5]. We measured the properties of the new $ErSi_{1.7}$ and $TbSi_{1.7}$ epitaxial layers.

For $YSi_{1.7}$, the Hall resistivity is positive at high temperatures, and decreases at low temperatures to negative values. The same trend occurs for $ErSi_{1.7}$ above 100 K (figure 8). This may be explained by a two-band model in a nearly compensated metal. The expression for Hall resistivity is then

$$R_H(T) = (\mu_p^2 n_p - \mu_e^2 n_e)/e(\mu_p n_p + \mu_e n_e)^2$$

where n_e and n_p are electron and hole densities and μ_e and μ_p their mobilities, functions of temperature.

For fitting purposes,the normal Hall resistivity will be approximated by the expression

$$R_H(T) = R_H^0(T) = \sqrt{(a + bT^2)} + c.$$

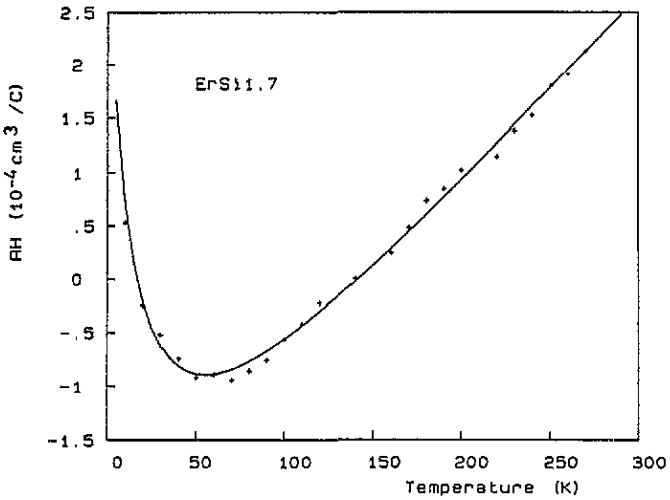

Figure 8. Hall resistivity for $ErSi_{1.7}$ film versus temperature in the paramagnetic range ($T_N = 4.5$ K). The continuous line is a fit incorporating the normal and anomalous Hall effect (see the text).

For magnetic materials, the Hall effect consists of two contributions, the normal one related to the density and mobility of carriers, and the anomalous Hall effect, which is related to the influence of the local moments on the conduction band. Various contributions to this term have been discussed by Berger [27] and Fert [28].

The temperature variation of R_H in $ErSi_{1.7}$ (figure 8) exhibits an upturn below 60 K, in contrast to the case of $YSi_{1.7}$; this feature can be accounted for by a normal term similar to that of $YSi_{1.7}$, plus a term proportional to the local 4f susceptibility.

In the present case of thin films, the demagnetizing field must be taken into account; the internal field is then

$$H_i = H_{appl} - 4\pi M = H_{appl}(1 - 4\pi X_{vol})$$

where X_{vol} is the susceptibility by volume unit.

Thus the Hall resistivity is obtained as

$$R_H(T) = R_H^0(T)[1 + \alpha 4\pi C_{vol}/(T - \Theta_p + 4\pi C_{vol})]$$

where the normal term is enhanced by the anomalous one, and α represents the coupling between the 4f shell susceptibility and conduction electron spins.

The fit in figure 8 is obtained from the above expression for $R_H^0(T)$, taking $a = 1.5 \times 10^{-10}$ cm^6 C^{-2}, $b = 3.4 \times 10^{-12}$ cm^6 C^{-2} K^{-2} and $c = -2.62 \times 10^{-4}$ cm^3 C^{-1}. C_{vol} is taken as the free Er^{3+} Curie constant divided by molar volume, Θ_p is about 5 K, as deduced from the susceptibility data with the field along the c axis, and $\alpha = -6.2$.

The negative sign of α means that the local field induced on the conduction band by the 4f polarization is opposite to that of the external field, which is in line with results for heavy rare earths.

In the case of $TbSi_{1.7}$ (figure 9),the same phenomenology may be applied. In this case however, the positive sign of R_H shows that we have dominant positive carriers at all temperatures, and $R_H^0(T)$ may be approximated by $R_H^0(T) = a + bT$, with

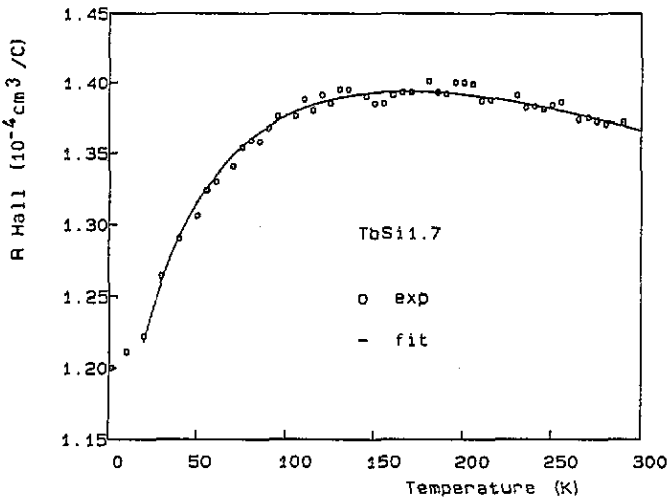

Figure 9. Hall resistivity and fit for $TbSi_{1.7}$ above $T_N = 33$ K (see the text).

$a = 1.6 \times 10^{-4}$ cm^3 C^{-1} and $b = -5.6 \times 10^{-8}$ cm^3 C^{-1} K^{-1}. At room temperature, the hole concentration is of the order of 8.5×10^{22} cm^{-3}. Once again, the anomalous term has a sign opposite to the normal one, with $\alpha = -3.3$.

In the low-temperature range, the Hall voltage V_H is no longer a linear function of H, due to the behaviour of the local magnetization (figure 10).

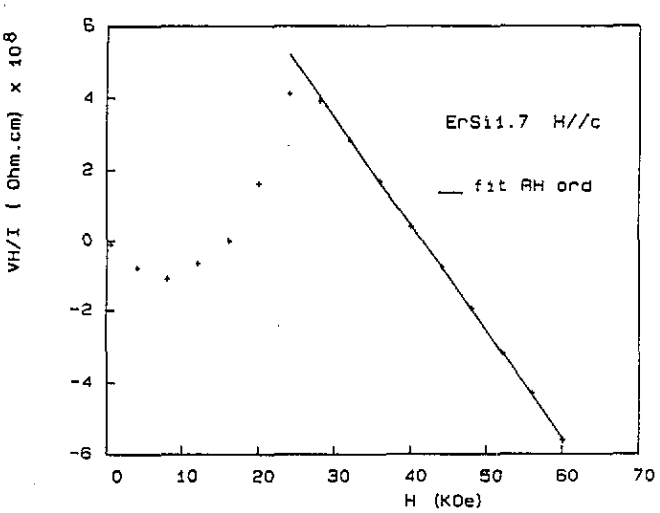

Figure 10. Hall resistance of $ErSi_{1.7}$ versus field. The slope of the continuous line gives the normal Hall resistivity.

Berger [27] and Fert [28] have shown that the anomalous Hall effect is the result of several mechanisms, such as skew scattering and side jump effects, related either to the spin or to the orbital moment of the 4f shell. It appears that the temperature dependence of the Hall effect may differ from that of the magnetization, especially for 3d metals, but that

the shape of isotherms for magnetization and Hall voltage should not be very different. We will assume that the anomalous term is proportional to the induction in the material, thus

$$V_H/I = R_H^0(T)H + R_H^a B(H,T).$$

In our case, it is possible to decompose the Hall voltage into normal and anomalous terms at low temperatures, as the magnetization of Er_3Si_5 saturates at about 2 T, after a metamagnetic behaviour at about 1.5 T. The normal term is then taken from the slope of the Hall voltage after saturation, and subtracted from the total signal. The anomalous Hall signal (figure 11) gives a good representation for the field dependence of the magnetization along the c axis, which is metamagnetic below the Néel point, and varies as a Brillouin function above.

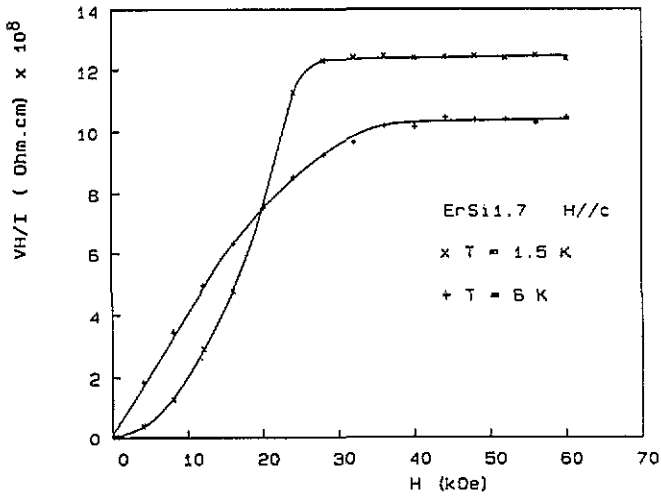

Figure 11. Anomalous Hall resistance, after subtraction of the normal term. The variations are similar to those of the magnetization for H perpendicular to the film [17].

Such a similar variation of Hall effect and magnetization may be useful, as measuring Hall effect allows us to study in a simple manner the qualitative behaviour of magnetization processes of very thin films. In this case, indeed, the magnetization itself is difficult to measure directly due to the small volume, even with SQUID or vibrating sample magnetometers, due to the importance of corrections from the sample holder and substrate.

6. Conclusion

From resistivity and Hall effect measurements, the rare earth silicides RSi_{2-x} may be characterized as nearly compensated metals.

The temperature and field behaviour of the resistivity can be accounted for in the paramagnetic or ordered states, using theoretical models that incorporate crystal field and exchange components. Magnetoresistance anomalies are associated with the metamagnetic behaviour in the ordered range. In particular, Ising like antiferromagnets, a sharp maximum of resistivity corresponds to the spin reversal on the downwards sublattice. These

measurements allow us to draw the phase diagram of metamagnetic samples and to verify the parameters included in the spin Hamiltonian.

The anomalous Hall effect could be separated from the normal term in Er and Tb compounds. In the paramagnetic range, it varies as the 4f susceptibility, the coupling between the 4f shell and the conduction electron spins being negative. In the ordered range, its field variation reproduces rather well the metamagnetic behaviour of the magnetization. Such similar variation is useful to study the qualitative behaviour of the magnetization for thin films.

Acknowledgment

This work has been sponsored by the Direction des Recherches et Moyens d'Essais (Direction Générale pour l'Armement).

References

[1] Bean J C and Poate J M 1980 *Appl. Phys. Lett.* **37** 643
Bean J C 1986 *Phys. Today* October p 36
[2] Rosencher E, Badoz P A, Pfister J C, Arnaud d'Avitaya F, Vincent G and Delage S 1986 *Appl. Phys. Lett.* **49** 271
[3] Cadoff I B and Miller E 1960 *Thermoelectric Materials and Devices* (London: Reinhold) p 163
[4] Knapp J A and Picraux S T 1986 *Appl. Phys. Lett.* **48** 466; 1986 *Proc. Met. Res. Soc. Symp.* **54** 261
[5] Duboz J Y, Badoz P A, Perio A, Oberlin J C, Arnaud d'Avitaya F, Campidelli Y and Chroboczek J A 1989 *Appl. Surf. Sci.* **38** 171
[6] Unewisse M H and Storey J W V 1992 *J. Appl. Phys.* **72** 2367
[7] Rogl P 1984 *Handbook on the Physics and Chemistry of Rare Earths* vol 7, ed K A Gschneidner and L Eyring (Amsterdam: North-Holland) p 1
[8] Houssay E, Rouault A, Thomas O, Madar R and Sénateur J P 1989 *Appl. Surf. Sci.* **38** 156
[9] Pierre J, Lambert-Andron B and Soubeyroux J L 1989 *J. Magn. Magn. Mater.* **81** 39
[10] Pierre J, Auffret S, Siaud E, Madar R, Houssay E, Rouault A and Sénateur J P 1990 *J. Magn. Magn. Mater.* **89** 86
[11] Auffret S, Pierre J, Lambert-Andron B, Soubeyroux J L and Chroboczek J A 1990 *Physics* B **162** 271
Auffret S, Pierre J, Lambert-Andron B, Madar R, Houssay E, Schmitt D and Siaud E 1991 *Physics* B **173** 265
[12] Schobinger-Papamentellos P, Janssen T, de Mooij D B and Buschow K H J 1990 *J. Less-Common Met.* **162** 197
[13] Houssay E 1990 *Thesis* Polytechnic Institute of Grenoble
Nava F, Tu K N, Thomas O, Sénateur J P, Madar R, Borghesi A, Guizzetti G, Gottlieb U, Laborde O and Bisi O 1993 *Mater Sci. Rep.* **9** 141
[14] Sato T and Ohtsuka T 1966 *Phys. Lett.* **20** 565
Sato T and Asada Y 1970 *J. Phys. Soc. Japan* **28** 263
[15] Lambert-Andron B, Sayetat F, Auffret S, Pierre J and Madar R 1991 *J. Phys.: Condens. Matter* **3** 3113
[16] Dijkman W H 1982 *PhD Thesis* University of Amsterdam
[17] Chroboczek J A, Briggs A, Joss W, Auffret S and Pierre J 1991 *Phys. Rev. Lett.* **66** 790
Auffret S, Pierre J, Chroboczek J A, Badoz P A, Arnaud d'Avitaya F, Guivarc'h A and Le Corre A 1992 *J. Magn. Magn. Mater.* **104–107** 1209
[18] Pierre J, Auffret S, Lambert-Andron B, Madar R, Murani A P and Soubeyroux J L 1992 *J. Magn. Magn. Mater.* **104** 1207
[19] van Peski-Tinbergen T and Dekker A J 1963 *Physica* **29** 917
[20] Fert A, Asomoza R, Sanchez D H, Spanjaard D and Friederich A 1977 *Phys. Rev.* B **16** 5040
[21] Elliott R J and Wedgwood F A 1963 *Proc. Phys. Soc.* **81** 846
Miwa H 1963 *Prog. Theor. Phys.* **29** 477
[22] Yamada H and Takada S 1973 *J. Phys. Soc. Japan* **34** 51

[23] Mackintosh A R and Spanel L E 1964 *Solid State Commun.* **2** 383
[24] de Gennes P G and Friedel J 1958 *J. Phys. Chem. Solids* **4** 71
[25] Allen S J, Tabatabaie N, Palmstrom C J, Hull G W, Sands T, DeRosa F, Gilchrist H L and Garrisson K C 1989 *Phys. Rev. Lett.* **62** 2309
[26] Pellissier A 1989 *Thesis* Polytechnic Institute of Grenoble
[27] Berger L 1970 *Phys. Rev.* B **2** 4559
[28] Fert A 1977 *Physica* B **86–88** 491